



Performance of solid-state Li-ion conducting battery using biopolymer electrolyte based on agar–agar/lithium chloride

S. Aafrin Hazaana^{1,2} · Ancemma Joseph¹ · S. Selvasekarapandian^{2,3} · R. Meera Naachiyar^{1,2} · N. Muniraj Vignesh^{2,4}

Received: 19 August 2022 / Revised: 31 October 2022 / Accepted: 29 November 2022 / Published online: 9 December 2022
© The Author(s), under exclusive licence to Springer-Verlag GmbH Germany, part of Springer Nature 2022

Abstract

In the present work, biopolymer electrolytes based on agar–agar (AA) and lithium chloride (LiCl) have been prepared using solution casting technique for the fabrication of better performing solid-state Li-ion conducting battery. X-ray diffraction (XRD) analysis has been carried out to analyse the crystalline/amorphous nature of the prepared membranes, and the membrane with the composition of 20 mol% of AA:80 mol% of LiCl shows high amorphous nature. Fourier transform infrared spectroscopy (FTIR) has been done to investigate the complex formation between the polymer and salt. The glass transition temperature (T_g) of all the prepared electrolytes has been examined using differential scanning calorimetry (DSC), and a low T_g value of 37 °C is observed for the membrane 20 mol% of AA:80 mol% of LiCl among all prepared electrolytes. AC impedance spectroscopy is carried out to calculate the ionic conductivity of prepared electrolytes, and the membrane with the concentration of 20 mol% of AA:80 mol% of LiCl exhibits a high ionic conductivity of $3.12 \pm 0.11 \times 10^{-2}$ S/cm. Surface analysis of prepared electrolytes has been carried out using scanning electron microscopy (SEM), and the thermal stability of prepared biopolymer membranes has been examined using thermogravimetric analysis (TGA). Cyclic voltammetry (CV) study is done for the highest Li-ion conducting membrane, and a good cyclic stability is observed. Subsequently, the electrolyte with high ionic conductivity (20 mol% of AA:80 mol% of LiCl) has been utilized in the fabrication of solid-state primary and secondary Li-ion conducting batteries.

Keywords Biopolymer · Agar–agar · Lithium chloride · AC impedance · Primary battery

Introduction

In the current age, necessity of energy storage devices has prompted the researchers to develop an unprecedented work towards better performing electrolytes which act as an essential part in electrochemical energy storage devices such as solid-state battery and so on [1]. Though liquid electrolytes are utilized in numerous works, solid electrolytes with considerable advantages act as a superior alternative

for aqueous/gel electrolytes [2]. Solid-state electrolytes are compact, safe, and ease to handle and result with fine contact between electrodes and electrolyte [3].

Among various solid-state electrolytes, polymer-based solid electrolytes play a vital role in the field of solid-state ionics due to its better film-forming nature [4]. Polymers are categorized based on its nature as synthetic and natural polymers. Enormous works have been carried out using synthetic polymers such as polyvinyl alcohol (PVA) [4], PVA-PAN [5], PEO [6], PVAc-PMMA [7] and many more as an electrolyte. But considering the consequence of few synthetic/petroleum-based polymers on environmental impact, the less-toxic, biodegradable, cost-effective and ample natured natural biopolymers are taken into account to behave as a host polymer in the present work. Few works executed with biopolymers such as gellan gum [8], sodium alginate [9], pectin [10], K/I-carrageenan [11, 12] and so on resulted with eminent efficiency and notable ionic conductivity.

Based on this perspective, agar–agar (AA) has been chosen as host material in the current study for the preparation

✉ S. Selvasekarapandian
sekarapandian@rediffmail.com

¹ Research Centre of Physics, Fatima College (Affiliated to Madurai Kamaraj University), Madurai 625018, India

² Materials Research Centre, Coimbatore 641045, India

³ Department of Physics, Bharathiar University, Coimbatore 641046, India

⁴ Department of Physics, Mannar Thirumalai Naicker College (Affiliated to Madurai Kamaraj University), Madurai 625004, India

of electrolyte. Agar–agar, extracted from red seaweed (*Rhodophyceae*), is formed by the mixture of two polysaccharides named agarose and agarpectin (refer to Fig. 1a) [13]. It has the existence of 3,6-anhydro-L-galactose as repeating units. Though both polysaccharides share galactose as backbone, agarpectin is heavily modified with acidic side groups such as sulphate and pyruvate and agarose is the low-sulphate, neutral gelling fraction of agar [14]. AA has marked its footsteps in medicinal field because of the presence of prebiotic fibres and minerals [15] along with incredible medicinal properties such as enhancing weight loss, preventing anaemia, strengthening bones, reducing cholesterol, regulating intestinal transit, treating cancer [16] and so on. Though AA has superior medicinal properties, it has been chosen as a host polymer for the preparation of electrolyte due to the presence of a substantial amount of polar groups to which a cation of any salt could be attached for better ionic conduction. In order to enhance the ionic conductivity, one of the simplest and best ways of adjoining ionic salts has been done. In this work, lithium chloride (LiCl), which has a small-sized cation (Li^+) in contrast to other alkali salts [16] and also showing remarkable solubility in polar solvents, has been selected to act as an additive in the polymer matrix to accomplish a better performing electrolyte for the fabrication of battery.

Few works carried out by researchers using biopolymers as host materials are pectin/LiCl with the ionic conductivity of 2.08×10^{-3} S/cm [17], I-carrageenan with LiCl showing the ionic conductivity of 5.33×10^{-3} S/cm [12] and gellan gum with LiCl resulting with better ionic conductivity of 4.08×10^{-3} S/cm [18], respectively. Though tremendous works are done using various biopolymers as host material in polymer matrix, as per literature review, no attempt has been done to prepare biopolymer electrolytes (BPEs) with AA as a chief polymer and LiCl as an additive.

In the current study, the development of AA-based BPEs incorporated with various concentrations of LiCl has been carried out using solution casting technique. The structural, vibrational, thermal, electrical and electrochemical

properties of prepared BPEs are characterized using various techniques such as X-ray diffraction (XRD), scanning electron microscopy (SEM), Fourier transform infrared spectroscopy (FTIR), differential scanning calorimetry (DSC), thermogravimetric analysis (TGA), AC impedance analysis, transference number measurement (TNM) and cyclic voltammetry (CV). At last, fabrication of Li-ion conducting primary and secondary (rechargeable) batteries has been done.

Experimental method

Solid BPEs with various compositions of AA and LiCl have been prepared using solution casting method (refer to Fig. 2). The total estimated weight is fixed as 1 g. Various weight percentages of AA and LiCl have been calculated to be 40 mol% of AA:60 mol% of LiCl, 30 mol% of AA:70 mol% of LiCl, 20 mol% of AA:80 mol% of LiCl and 10 mol% of AA:90 mol% of LiCl, respectively. The calculated mol% of AA is added pinch by pinch in hot water maintained at the temperature of about 85°C and allowed to stir well for 2 h. Then, the obtained clear solution has been incorporated with different weight percentages (60 mol%, 70 mol%, 80 mol% and 90 mol%) of LiCl and the solution is stirred well for 2 h again. Finally, the obtained homogeneous solution is poured in a polypropylene Petri dish placed at the hot plate fixed with the temperature of 45°C . After 24 h, flexible and transparent films have been obtained with the thickness ranging from 0.15 to 0.25 mm.

Characterization techniques

Structural analysis

The crystalline/amorphous nature of the electrolytes prepared is analysed using X-ray diffraction method with a Philips X'Pert Diffractometer using the source of Cu/K α radiation in the wavelength of 1.54 \AA with the scan rate of $5\text{--}80^\circ$ at ambient temperature [8].

Fig. 1 a Chemical structure of agar–agar. b Possible interaction of LiCl with the biopolymer (agar–agar)

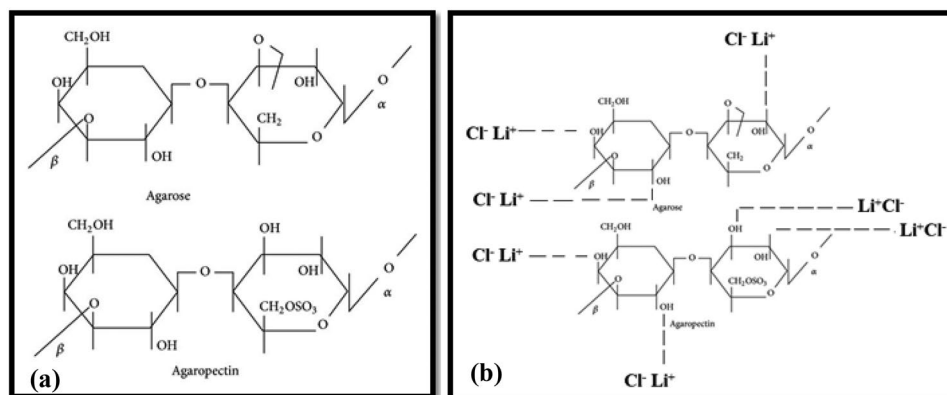
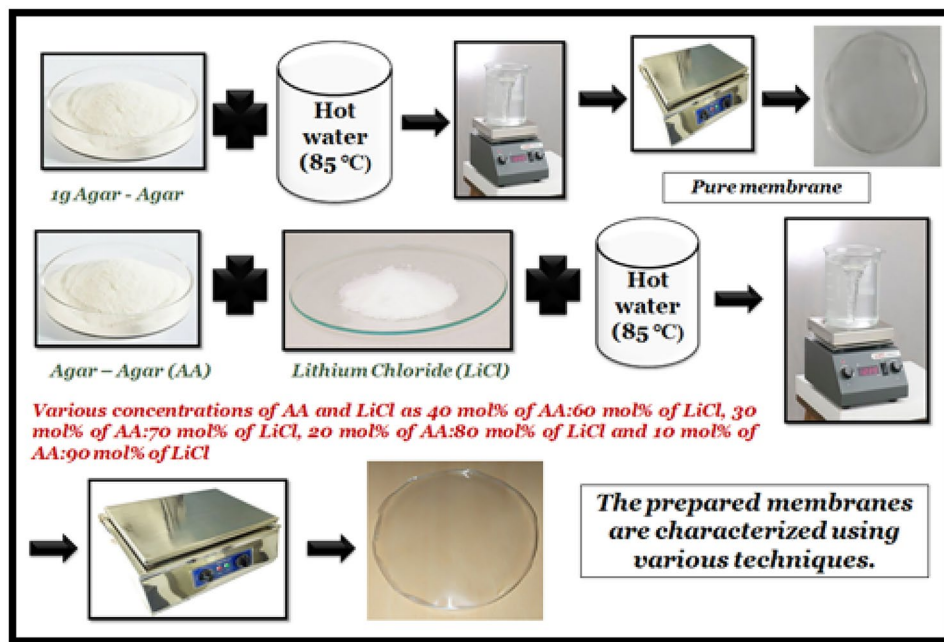


Fig. 2 Scheme of preparation of BPEs based on agar-agar with LiCl



Vibrational analysis

Fourier transform infrared spectroscopy has been carried out using Shimadzu IRAffinity-1 in the frequency range of 500–4000 cm^{-1} with a resolution of 1 cm^{-1} to confirm the complex formation between the polymer and the salt [18].

Thermal analysis

Differential scanning calorimetry is done with DSC Q20 V4 under the nitrogen atmosphere at the heating rate of 10 $^{\circ}\text{C}/\text{min}$ to observe the glass transition temperature of the prepared membranes [18].

AC impedance analysis

The ionic conductivity of the prepared BPEs has been measured using a Hioki HiTester LCR meter with the frequency range of 42 Hz–5 MHz at the room temperature [8]. The bulk conductivity is examined from Nyquist plots using Boukamp software.

Surface morphology analysis

Surface analysis of prepared biopolymer membranes has been analysed using a JEOL JSM-6390 Scanning Electron Microscope [39].

Thermogravimetric analysis

Thermal stability of the prepared biopolymer electrolytes has been examined using DSC-TGA standard (SDT Q600 V20.9 Build 20) under nitrogen atmosphere at a flow rate of 200 ml/min. The samples are heated from 30 to 700 $^{\circ}\text{C}$ at the heating range of 10 $^{\circ}\text{C}/\text{min}$ and a weight of the sample around ~2.5 mg [39].

Analysis of ion transportation

Wagner's polarization method

Using Wagner's polarization method, the nature of charge carriers in the highest ion conducting membrane has been identified. The prepared BPE is placed between the stainless steel electrodes, and a small amount of DC voltage (1 V) is applied to the electrodes. Then, the variation of DC current is observed with respect to time [7].

Evan's polarization method

The transference number of cations in the prepared high ion conducting electrolyte has been measured using Evan's polarization method along with impedance spectroscopy to analyse the polarization effect. The electrolyte with high ionic conductivity is sandwiched between two silver electrodes with the configuration of silver electrode (X) || 20 mol% of AA:80 mol% of LiCl (highest ion conducting membrane) || silver electrode (X) [19].

Electrochemical analysis

Cyclic voltammetry

The electrochemical stability of the optimized highest ion conducting electrolyte (20 mol% of AA:80 mol% of LiCl) has been examined using CHI600C Series Electrochemical Analyser under the potential range fixed with -1 to $+1$ V at the scan rate of 0.1 V/s [18].

Application of prepared electrolyte

Fabrication of Li-ion conducting primary battery

Preparation of anode

To prepare anode, zinc dust powder (Zn), zinc sulphate heptahydrate ($\text{ZnSO}_4 \cdot 7\text{H}_2\text{O}$) and graphite (C) have been taken in the appropriate ratio of 8:2:1 and ground well for several hours. Then, the obtained mixture is made into thin pellets using a hydraulic press machine [11].

Preparation of cathode

Cathode is prepared with the composition of lead oxide (PbO_2), vanadium pentoxide (V_2O_5) and graphite (C) taken in the suitable ratio of 3:1:1 and ground well for several hours. The resulting mixture is placed in a hydraulic press machine to make thin pellets [12].

Fabrication of primary battery

The optimized highest Li-ion conducting electrolyte (20 mol% of AA:80 mol% of LiCl) is placed between the electrodes (anode and cathode) made into pellets with the configuration of $\text{Zn} + \text{ZnSO}_4 \cdot 7\text{H}_2\text{O} + \text{C}$ (as anode) || highest Li^+ ion conducting membrane (as electrolyte) || $\text{PbO}_2 + \text{V}_2\text{O}_5 + \text{C} + \text{BPE}$ (as cathode) under the room temperature. The resulting open-circuit voltage (OCV) has been noted, and the performance of the cell has been examined.

Fabrication of rechargeable Li-ion conducting cell

Preparation of anode

Anode is prepared with the suitable amount of graphite powder (3 g) which is made into slurry using a binder solution (*N*-methyl-2-pyrrolidone (NMP) solution + PVA) as a solvent. The prepared slurry has been coated over copper foil using doctor blade method and allowed to dry under the temperature of 70 °C in the vacuum oven for few hours. The coated and dried Cu foil is calendered to obtain the uniform

contact area. Finally, the anode foil is cut into 12 mm diameter with the mass of 0.116 g.

Preparation of cathode

To prepare cathode, lithium iron phosphate (LiFePO_4) (3 g) and graphite (1 g) with the suitable ratio of 3:1 are made into slurry with a binder solution (NMP solution + PVA) as a solvent. The obtained slurry is coated over the aluminium foil using doctor blade method and placed in the vacuum oven under the temperature of 70 °C for few hours. Subsequently, the dried foil has been calendered to have the uniform contact area. Then, the Al foil cathode with the mass of 0.104 g is cut into 12 mm diameter.

Fabrication of rechargeable Li-ion conducting cell

The cell has been fabricated with the prepared anode and cathode along with the highest Li-ion conducting membrane (20 mol% of AA:80 mol% of LiCl) and arranged with the configuration of graphite (C) || highest Li-ion conducting membrane || $\text{LiFePO}_4 + \text{C}$. The setup is well tightened in order to ensure the uniform and solid contact between the electrode and electrolyte.

Performance study of the cell

The fabricated cell is placed inside the battery holder, and the initial voltage has been noted. Impedance measurement is also taken before charging. Then, the cell is allowed to charge for 3 h with the DC voltage of 3 V and the initial output voltage is recorded. Then, the charged cell undergoes self-discharge for 2 h. This process of charging and discharging is repeated for 5 cycles. After the completion of 5 cycles, impedance measurement is taken for the cell. Again, the process continues for 5 more cycles. After the 10th cycle (i.e. from the 11th cycle), the cell is charged and discharged through a load of 100 K Ω . Simultaneously, while discharging, the current is also drawn from the cell and noted. The same work has been done by Venkata Jyotsna et al. [20] for the triblock polymer poly(vinylidene chloride-co-acrylonitrile-co-methyl methacrylate) with LiClO_4 and by Arockia Mary et al. [21] for the biopolymer kappa-carrageenan with LiCl.

Results and discussion

Structural analysis (X-ray diffraction method)

X-ray diffraction method has been carried out to analyse the crystalline/amorphous nature of the prepared BPEs. Figure 3a depicts the XRD pattern of pure agar and agar incorporated with various compositions of LiCl (40 mol%

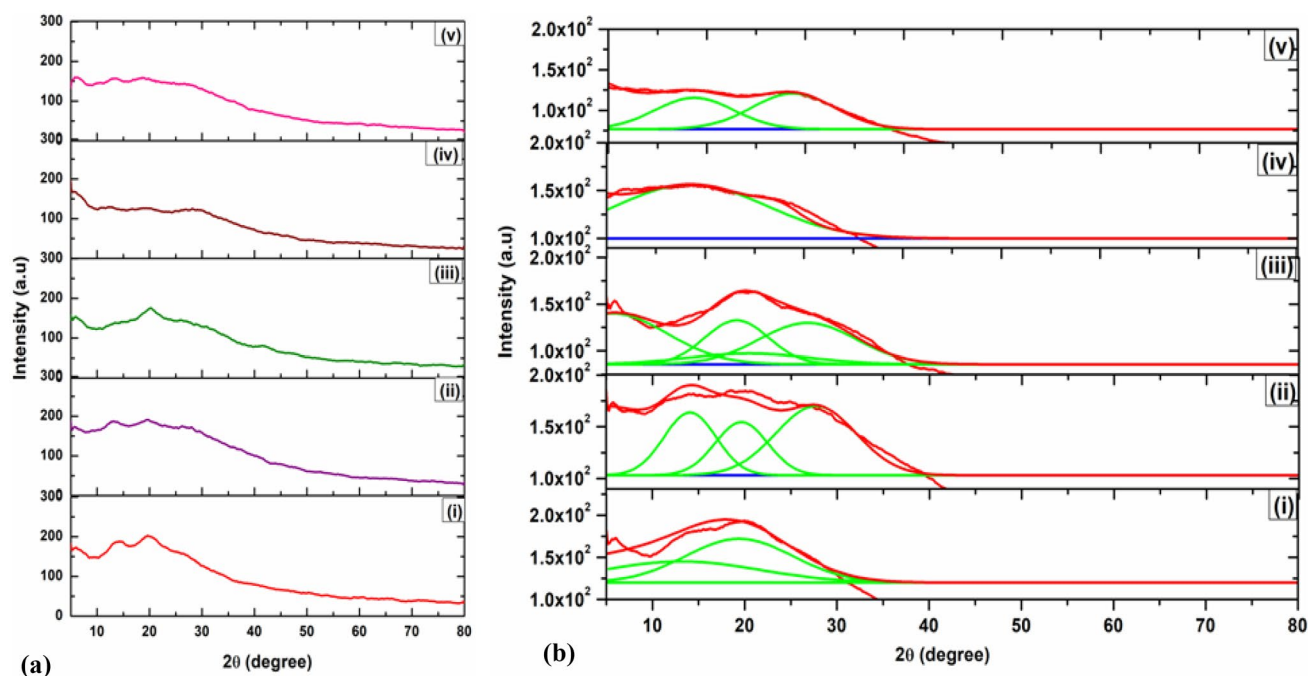


Fig. 3 **a** XRD and **b** deconvoluted XRD patterns of (i) pure agar (AA) (1 g), (ii) 40 mol% of AA:60 mol% of LiCl, (iii) 30 mol% of AA:70 mol% of LiCl, (iv) 20 mol% of AA:80 mol% of LiCl and (v) 10 mol% of AA:90 mol% of LiCl

of AA:60 mol% of LiCl, 30 mol% of AA:70 mol% of LiCl, 20 mol% of AA:80 mol% of LiCl and 10 mol% of AA:90 mol% of LiCl). From the semi-crystalline peak

percentage of the prepared BPEs has been determined using the following formula with deconvoluted XRD patterns:

$$\text{Percentage of crystallinity (\%C)} = \frac{\text{Area under crystalline region}}{\text{Total area of the peak}} \times 100\% \quad (1)$$

of pure agar represented in Fig. 3a(i), the peak positions are observed at 13° and 20° , which is in accordance with Boopathi et al. [22]. With the addition of LiCl, the broadness of peak increases and intensity decreases with the increase in salt concentration. From Fig. 3a(ii–v), it is assured that the membrane with the composition of 20 mol% of AA:80 mol% of LiCl shows high amorphous nature with less intensity and increased broadness of peak in contrast to other prepared membranes. It is to be noted that the peaks 13° and 20° have been suppressed completely in the membrane 20 mol% of AA:80 mol% of LiCl, and it shows a modest increase in the electrolyte with the concentration of 10 mol% of AA:90 mol% of LiCl which is due to the aggregates of ion in the polymer matrix leading to the increase in crystalline nature.

The obtained results for intensity and broadness of the diffraction peaks are correlated with Hodge et al.'s [23] criterion. It is noted that the peak due to LiCl is not observed in salt-added membranes which indicates the complete dissociation of the salt. The crystalline

The calculated crystalline percentage of prepared BPEs is tabulated in Table 1. Figure 3b depicts the deconvoluted XRD pattern of pure agar and agar incorporated with various concentrations of LiCl (40 mol% of AA:60 mol% of LiCl, 30 mol% of AA:70 mol% of LiCl, 20 mol% of AA:80 mol% of LiCl and 10 mol% of AA:90 mol% of LiCl). From Table 1, it is observed that pure agar results with the crystalline percentage of 63% and the electrolyte with the concentration of 20 mol% of AA:80 mol% of LiCl

Table 1 Crystallinity percentage of prepared BPEs

Composition	Crystallinity percentage (%C)
Pure agar (AA) (1 g)	63
40 mol% of AA:60 mol% of LiCl	56
30 mol% of AA:70 mol% of LiCl	36
20 mol% of AA:80 mol% of LiCl	15
10 mol% of AA:90 mol% of LiCl	25

is inferred with a less crystalline percentage of 15% C in contrast to other salt-added membranes. And on further addition of salt (10 mol% of AA:90 mol% of LiCl), the crystallinity percentage increases which assures the formation of clusters in polymer matrix.

Vibrational analysis (Fourier transform infrared spectroscopy)

Fourier transform infrared spectroscopy has been carried out to assure the complex formation between the host polymer and the salt. Figure 4 represents the FTIR spectrum of all prepared biopolymer electrolytes (40 mol% of AA:60 mol% of LiCl, 30 mol% of AA:70 mol% of LiCl, 20 mol% of AA:80 mol% of LiCl and 10 mol% of AA:90 mol% of LiCl). The vibrational peaks with the spectral band assignments of all prepared biopolymer electrolytes are ascribed in Table 2.

From Table 2, it is to be noted that the vibrational peak positions of pure agar at 886 cm^{-1} , 930 cm^{-1} , 1036 cm^{-1} , 1151 cm^{-1} , 1370 cm^{-1} , 1639 cm^{-1} and 2923 cm^{-1} peaks do not undergo much changes in frequency with the addition of salt. But, the peak position at 3365 cm^{-1} attributed to OH stretching

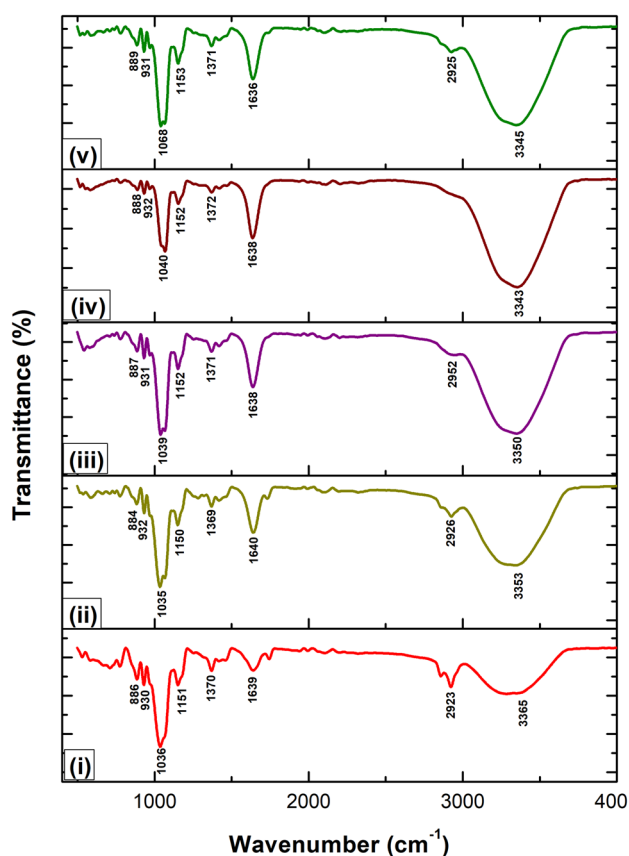


Fig. 4 FTIR spectrum of (i) pure agar (AA) (1 g), (ii) 40 mol% of AA:60 mol% of LiCl, (iii) 30 mol% of AA:70 mol% of LiCl, (iv) 20 mol% of AA:80 mol% of LiCl and (v) 10 mol% of AA:90 mol% of LiCl

gets a frequency decrease with an increase in salt concentration. This decreased change in frequency in OH stretching is due to the interaction between the oxygen of OH⁻ group and Li⁺ of incorporated lithium salt (LiCl) which confirms the complex formation between the polymer and the salt.

The intensity of peaks at 886 cm^{-1} and 930 cm^{-1} gets decreased as the concentration of salt increases up to 80 mol% of LiCl. This again indicates the complex formation between the polymer and salt. The intensity of broad peak at 1639 cm^{-1} increases with the addition of salt, and the broadness decreases and becomes sharp with an increase in the concentration of salt. The intensity of the peak at 2923 cm^{-1} decreases with an increase in the concentration of salt and is completely absent for the concentration 80 mol% of LiCl. On further increase in salt concentration, the peak appears again with small intensity. This also confirms the complex formation between the host polymer and the salt.

The broad characteristic peak at 3365 cm^{-1} in pure agar which attributes to OH stretching [22] has been shifted to 3353 cm^{-1} , 3350 cm^{-1} , 3343 cm^{-1} and 3345 cm^{-1} for the membrane with the composition of 40 mol% of AA:60 mol% of LiCl, 30 mol% of AA:70 mol% of LiCl, 20 mol% of AA:80 mol% of LiCl and 10 mol% of AA:90 mol% of LiCl, respectively. This decreased change in frequency in OH stretching is due to the interaction between the oxygen of OH⁻ group and Li⁺ of incorporated lithium salt (LiCl) which assures the better complex formation between the polymer and the salt.

Thus, the slight shift in peaks, the variation in frequency and intensity and the absence of vibrational peaks ensure the complex formation between the host biopolymer (agar-agar) and the salt (LiCl) added. Figure 1b represents the possible interaction of LiCl with the host biopolymer (agar-agar).

The change in frequency could be understood by calculating the force constant (k).

The force constant (k) has been calculated using Hooke's relation [18]

$$\nu = \frac{1}{2\pi c} \sqrt{\frac{k}{\mu}} \text{ N/cm} \quad (2)$$

where $\mu = \frac{m_1 \times m_2}{m_1 + m_2}$ gives the reduced mass. The force constant is calculated for O–H stretching and is tabulated in Table 3. From Table 3, we can observe that as the concentration of salt increases, the force constant decreases which leads to an increase in bond length. As the bond length increases, there is a decrease in vibrational frequency which assures the better complex formation between the polymer and salt.

Thermal analysis (Differential scanning calorimetry)

DSC has been done to determine the glass transition temperature (T_g) of prepared BPEs. Figure 5 ascribes the DSC thermograms of prepared membranes. Table 4 depicts the T_g

Table 2 Vibrational peak with the spectral band assignments of all prepared biopolymer electrolytes

Pure agar (AA) (1 g)	40 mol% of AA:60 mol% of LiCl	30 mol% of AA:70 mol% of LiCl	20 mol% of AA:80 mol% of LiCl	10 mol% of AA:90 mol% of LiCl	Assignment	Reference
886	884	887	888	889	Skeletal mode of β -D-galactose units	[24]
930	932	931	932	931	C–O–C stretching of 3,6-anhydrogalactose	[24, 25]
1036	1035	1039	1040	1068	C–O or C–C stretching of pyranose ring	[18, 26]
1151	1150	1152	1152	1153	Ester-sulphate link vibration	[24, 27]
1370	1369	1371	1372	1371	CH ₂ in plane bending	[22]
1639	1640	1638	1638	1636	Amide-I vibration	[24]
2923	2926	2952	–	2925	CH ₂ stretching	[18, 24]
3365	3353	3350	3343	3345	OH stretching	[22]

value of all prepared BPEs with various salt compositions. From Table 4, it is observed that as the concentration of salt increases, the T_g value decreases which may enhance the flexibility of the electrolyte and may pave a way for better ion conduction [31]. The DSC pattern of pure agar represented in Fig. 5(i) shows a T_g value of 53 °C. In contrast to other prepared membranes, the electrolyte with the composition of 20 mol% of AA:80 mol% of LiCl exhibits a low T_g value of 37 °C which may be due to the plasticizing effect of the salt and the weak transient cross linkage between the polymer and salt. On further addition of salt, the membrane 10 mol% of AA:90 mol% of LiCl results with an increased value of T_g as 41 °C, indicating that the transient cross linkage becomes a little bit strong between the polymer and salt [19]. Related observations are reported by Arockia Mary et al. [11] for the biopolymer K-carrageenan with LiNO₃ and by Perumal et al. [17] for the polymer pectin with LiCl.

AC impedance analysis

AC impedance analysis has been performed to measure the ionic conductivity of all prepared BPEs using Cole–Cole plots over a wide range of frequencies at ambient temperature. Figure 6 ascribes the Cole–Cole plots of (i) pure agar, (ii) 40 mol% of AA:60 mol% of LiCl, (iii) 30 mol% of AA:70 mol% of LiCl, (iv) 20 mol% of AA:80 mol% of LiCl and (v) 10 mol% of AA:90 mol% of LiCl, respectively. The

Cole–Cole plots are usually obtained with a high-frequency semicircle and an inclined spike at a low-frequency region. Figure 6(i) representing the plot of pure agar is inferred with a semicircle (due to immobile polymer chains) indicating the capacitance nature of an electrolyte. The plots of 40 mol% of AA:60 mol% of LiCl, 30 mol% of AA:70 mol% of LiCl, 20 mol% of AA:80 mol% of LiCl and 10 mol% of AA:90 mol% of LiCl mentioned in Fig. 6(ii–v) are observed with an inclined spike representing the resistive nature of an electrolyte (due to the migration of ions) along with constant phase element which may be due to the formation of double-layer capacitance at the electrode–electrolyte interface [28]. The bulk resistance has been calculated using impedance plots with EQ Boukamp software [29]. Ionic conductivity has been calculated using the formula

$$\sigma = \frac{l}{AR_b} \quad (3)$$

where l is the thickness, A is the area and R_b is the bulk resistance of the analysed BPEs. Electrochemical impedance spectroscopy (EIS) parameters and ionic conductivity of all prepared electrolytes are tabulated in Tables 5 and 6.

The impedance of constant phase element is represented by the following equation [18]:

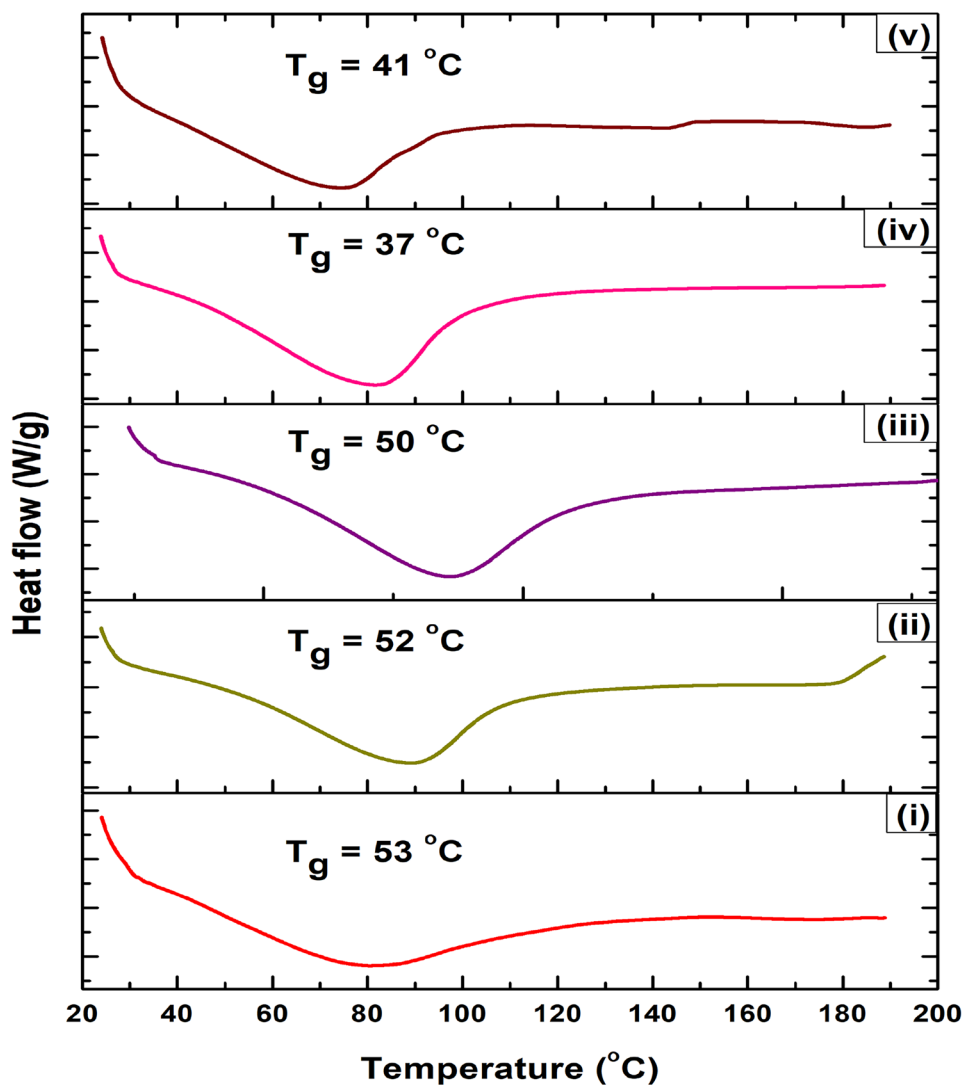
$$Z_{CPE} = \frac{1}{Q_0(j\omega)^n} \quad (4)$$

where Q_0 and n are frequency-independent parameters and the n value ranges from 0 to 1. It represents a pure capacitor if $n=1$ and if $n=0$, and it indicates a pure resistor. The bulk resistance value of pure agar is 217,435 Ω , and the salt-added membranes with the composition of 40 mol% of AA:60 mol% of LiCl, 30 mol% of AA:70 mol% of LiCl, 20 mol% of AA:80 mol% of LiCl and 10 mol% of AA:90 mol% of LiCl give a R_b value of 8.526 Ω , 2.477 Ω , 0.306 Ω and 1.265 Ω , respectively. The constant phase element (CPE) value of pure agar is 4.45×10^{-8} μF , whereas with the addition of LiCl, the CPE value varies as 3.57×10^{-4}

Table 3 Force constant for O–H stretching

Polymer composition	O–H stretching	
	Wave number (cm ⁻¹)	Force constant (N/cm)
Pure agar (AA) (1 g)	3365	627.92
40 mol% of AA:60 mol% of LiCl	3353	623.44
30 mol% of AA:70 mol% of LiCl	3350	622.34
20 mol% of AA:80 mol% of LiCl	3343	619.44
10 mol% of AA:90 mol% of LiCl	3345	620.58

Fig. 5 DSC thermograms of (i) pure agar (AA) (1 g), (ii) 40 mol% of AA:60 mol% of LiCl, (iii) 30 mol% of AA:70 mol% of LiCl, (iv) 20 mol% of AA:80 mol% of LiCl and (v) 10 mol% of AA:90 mol% of LiCl



μF (40 mol% of AA:60 mol% of LiCl), $2.97 \times 10^{-4} \mu\text{F}$ (30 mol% of AA:70 mol% of LiCl), $1.62 \times 10^{-4} \mu\text{F}$ (20 mol% of AA:80 mol% of LiCl) and $1.77 \times 10^{-4} \mu\text{F}$ (10 mol% of AA:90 mol% of LiCl), respectively. Then, pure agar (AA) results with the n value of 0.7180 and the electrolytes with the composition of 40 mol% of AA:60 mol% of LiCl, 30 mol% of AA:70 mol% of LiCl, 20 mol% of AA:80 mol%

of LiCl and 10 mol% of AA:90 mol% of LiCl exhibit the n value of 0.6821, 0.6292, 0.4579 and 0.5843, respectively.

From Table 6, it is observed that the ionic conductivity of pure agar (AA) is $9.80 \pm 0.12 \times 10^{-8} \text{ S/cm}$. Then, with the addition of various concentrations of LiCl, the ionic conductivity has been enhanced further. Among all salt-added membranes, the electrolyte with the composition of 20 mol% of AA:80 mol% of LiCl exhibits a high ionic conductivity of $3.12 \pm 0.11 \times 10^{-2} \text{ S/cm}$. On further addition of salt (10 mol% of AA:90 mol% of LiCl), the value of ionic conductivity is decreased to $7.57 \pm 0.18 \times 10^{-3} \text{ S/cm}$ which may be because of the aggregation/agglomeration of ions in the polymer network. Few works based on BPEs with lithium-based ionic salts as an additive for better ionic conductivity are as follows: iota-carrageenan with LiCl showing an ionic conductivity of $5.33 \times 10^{-3} \text{ S cm}^{-1}$ at room temperature by Chitra et al. [12], pectin/LiClO₄ resulting with $5.15 \times 10^{-5} \text{ S cm}^{-1}$ ionic conduction at room

Table 4 Glass transition temperature (T_g) of all prepared membranes

Composition	Glass transition temperature (T_g) (°C)
Pure agar (AA) (1 g)	53
40 mol% of AA:60 mol% of LiCl	52
30 mol% of AA:70 mol% of LiCl	50
20 mol% of AA:80 mol% of LiCl	37
10 mol% of AA:90 mol% of LiCl	41

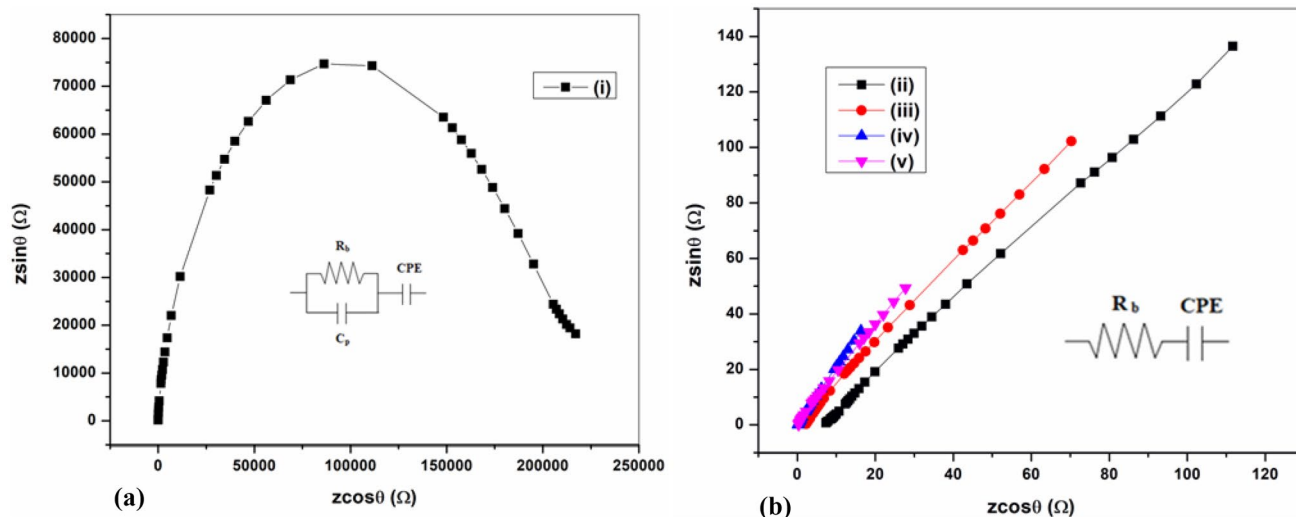


Fig. 6 Cole–Cole plots of **a** (i) pure agar (AA) (1 g) and **b** (ii) 40 mol% of AA:60 mol% of LiCl, (iii) 30 mol% of AA:70 mol% of LiCl, (iv) 20 mol% of AA:80 mol% of LiCl and (v) 10 mol% of AA:90 mol% of LiCl

temperature [30] and tamarind seed polysaccharide with LiCF_3SO_3 done by Kumar et al. [31] which has been optimized with a high ionic conductivity of $8.37 \times 10^{-4} \text{ S cm}^{-1}$ at ambient temperature.

Conductance spectra

Figure 7 shows the conductance spectra of all prepared biopolymer electrolytes (i) pure agar (AA), (ii) 40 mol% of AA:60 mol% of LiCl, (iii) 30 mol% of AA:70 mol% of LiCl, (iv) 20 mol% of AA:80 mol% of LiCl and (v) 10 mol% of AA:90 mol% of LiCl). Generally, conductance spectra consist of three different regions, namely the low-frequency dispersion region which indicates the space-charge polarization at the blocking electrodes, the mid-frequency region which depicts the DC ionic conductivity of the prepared BPEs which may be due to the migration of ions to the neighbouring sites and the high-frequency region which represents the bulk relaxation process [18]. In the present work, the pattern consists

of low-, mid- and high-frequency regions for pure agar whereas the salt-added membranes comprise of low- and mid-frequency regions. The DC ionic conductivity is calculated by extrapolating the mid-frequency-independent plateau region to zero frequency ($\log \sigma$ -axis). The logarithmic conductivity value obtained for the highest ion conducting membrane with the composition of 20 mol% of AA:80 mol% of LiCl is -1.8209 . The ionic conductivity resulted from conductance spectra ($1.46 \times 10^{-2} \text{ S/cm}$) is in resemblance with ionic conductivity obtained using Cole–Cole plots ($3.12 \times 10^{-2} \text{ S/cm}$).

Surface morphology analysis (SEM)

The surface morphology of prepared biopolymer electrolytes is analysed using SEM. Figure 8 represents the SEM image of (a) pure agar membrane (1 g), (b) 20 mol% of AA:80 mol% of LiCl (highest ion conducting membrane) and (c) 10 mol% of AA:90 mol% of LiCl, respectively.

From Fig. 8a, it is observed that the pure agar (AA) membrane results with a non-porous surface without any phase separation and the presence of small cube-shaped grains indicates the semi-crystalline nature of the polymer

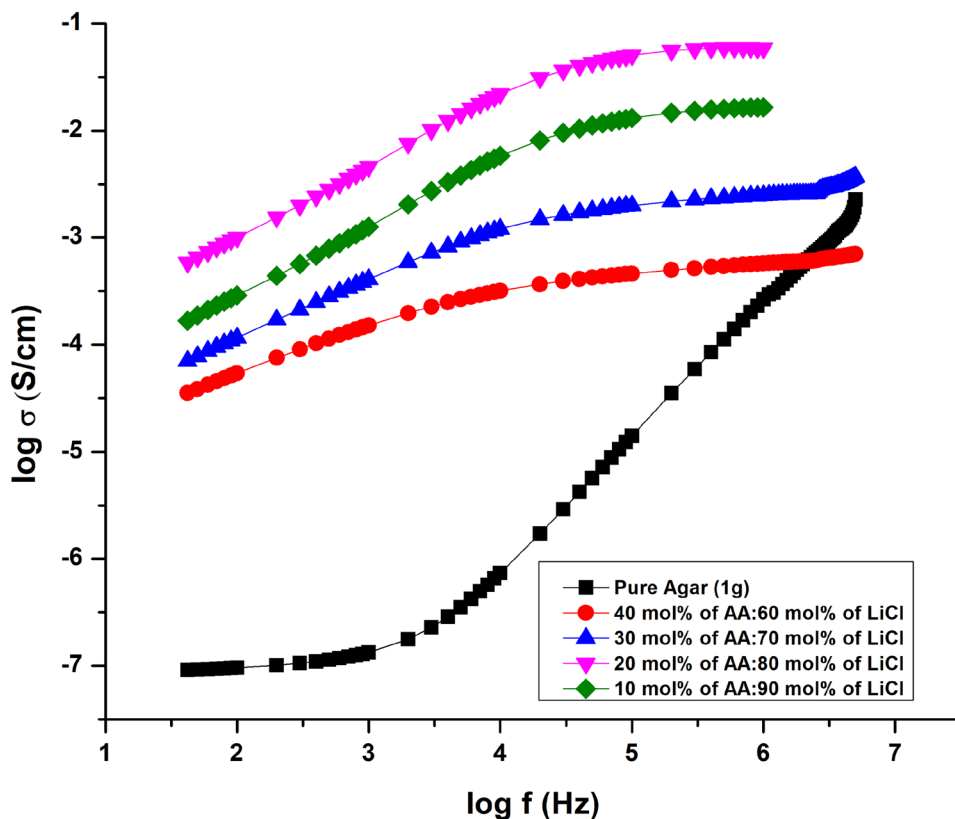
Table 5 Electrochemical impedance spectroscopy (EIS) parameters of all prepared BPEs

Composition	Bulk resistance (R_b) (Ω)	CPE (μF)	n (no unit)
Pure agar (AA) (1 g)	217,435	4.45×10^{-8}	0.7180
40 mol% of AA:60 mol% of LiCl	8.526	3.57×10^{-4}	0.6821
30 mol% of AA:70 mol% of LiCl	2.477	2.97×10^{-4}	0.6292
20 mol% of AA:80 mol% of LiCl	0.306	1.62×10^{-4}	0.4579
10 mol% of AA:90 mol% of LiCl	1.265	1.77×10^{-4}	0.5843

Table 6 Ionic conductivity calculated for all prepared electrolytes

Composition	Ionic conductivity (S/cm)
Pure agar (AA) (1 g)	$9.80 \pm 0.12 \times 10^{-8}$
40 mol% of AA:60 mol% of LiCl	$4.60 \pm 0.17 \times 10^{-4}$
30 mol% of AA:70 mol% of LiCl	$1.99 \pm 0.14 \times 10^{-3}$
20 mol% of AA:80 mol% of LiCl	$3.12 \pm 0.11 \times 10^{-2}$
10 mol% of AA:90 mol% of LiCl	$7.57 \pm 0.18 \times 10^{-3}$

Fig. 7 Conductance spectra of prepared BPEs



[32]. Thereafter, various concentrations of LiCl have been added to pure AA, whereas the presence of the LiCl on the membrane surface is clearly visible which is evenly distributed across the films (refer to Fig. 8b) [33].

Then, in Fig. 8b, it is clearly examined that the membrane with the composition of 20 mol% of AA:80 mol% of LiCl exhibits a smooth homogeneous surface with the absence of small cube-shaped grains observed in AA. This indicates the high amorphous nature and possibility of better polymer-salt complex resulting with high ionic conductivity [34].

Further on increasing the salt concentration, the SEM image of the membrane 10 mol% of AA:90 mol% of LiCl shows aggregates of ions (cluster formation). This assures the increase in crystallinity nature (refer to Table 1) and the decrease in ionic conductivity (refer to Table 6) of the membrane [35].

Thermogravimetric analysis

Thermal stability of prepared biopolymer electrolytes has been examined using TGA. Figure 9 ascribes the thermogravimetric analysis of (a) pure agar (AA) and (b) 20 mol% of AA:80 mol% of LiCl (highest ion conducting membrane).

By analysing Fig. 9, it is examined that the first stage of degradation occurs at 40 to 240 °C for pure agar (Fig. 9a)

and at 30 to 180 °C for 20 mol% of AA:80 mol% of LiCl membrane (Fig. 9b) with the weight loss of 19.4% (AA) and 37.3% (20 mol% of AA:80 mol% of LiCl), respectively. This first stage of weight loss and degradation is due to the elimination of moisture content in the membrane [36].

Then, the second stage of degradation occurs for AA (Fig. 9a) at 240 to 700 °C with the weight loss of 58.6% which may be because of the destruction of backbone polysaccharides such as agarose and agarpectin [37]. Similarly, the second stage of degradation at 180 to 690 °C with the weight loss of 30.5% for 20 mol% of AA:80 mol% of LiCl is due to the polymer-salt matrix destruction [38, 39].

The polymer membrane suffers an endothermic reaction of oxidation and hydrolysis, subsequently the exothermic reaction of polysaccharide pyrolysis during the degradation process [40]. The remaining residue of AA is 15.5%, and that of 20 mol% of AA:80 mol% of LiCl is 25.8%.

Analysis of ion transportation (transference number measurement)

Wagner's polarization technique

Wagner's polarization method is performed to measure the transference number of ions (t_{ion}) and electrons (t_{elec}) in the highest ion conducting membrane. The membrane with the

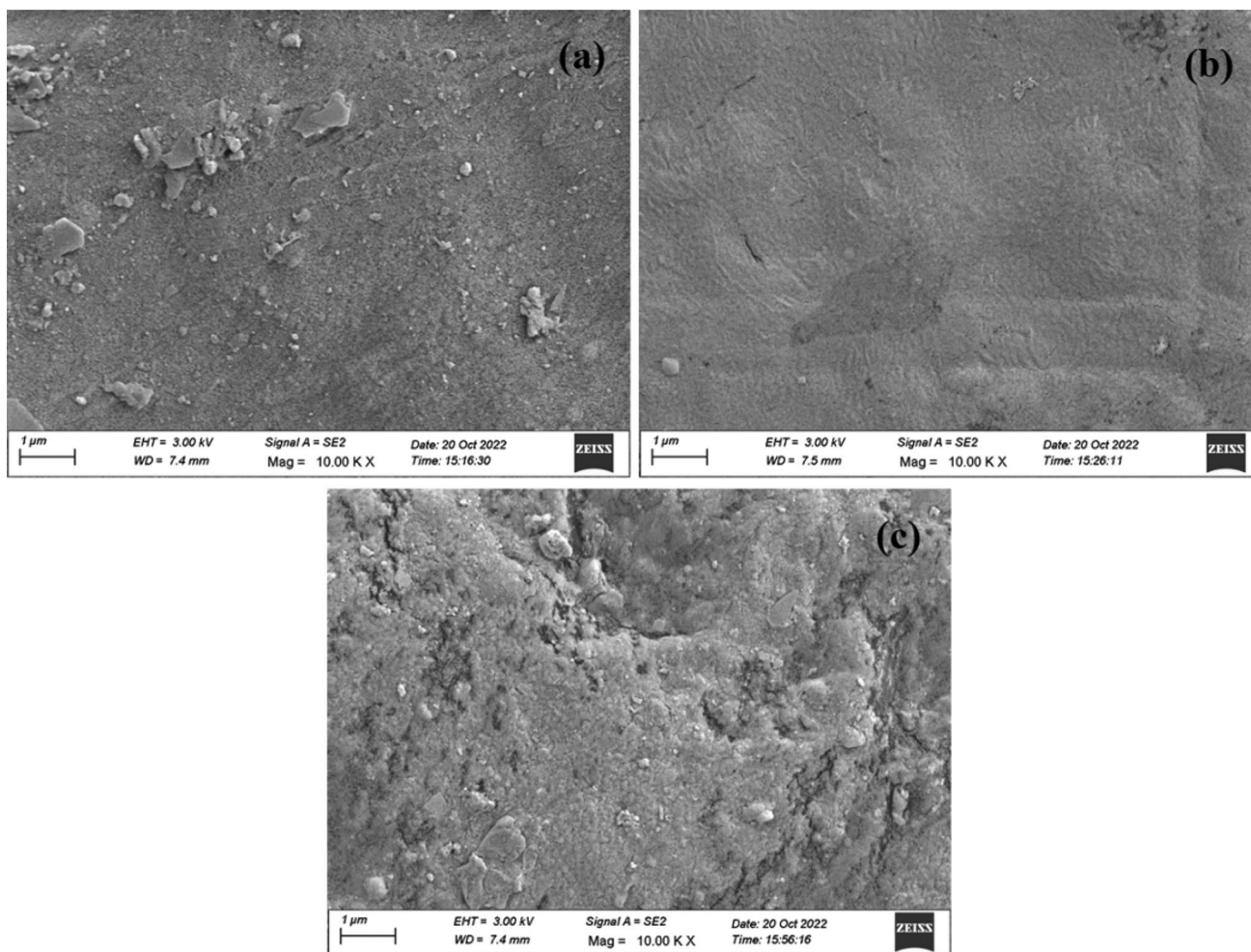


Fig. 8 SEM image of (a) pure agar membrane (AA) (1 g), (b) 20 mol% of AA:80 mol% of LiCl and (c) 10 mol% of AA:90 mol% of LiCl

composition of 20 mol% of AA:80 mol% of LiCl (highest ion conducting membrane) is placed between two stainless steel electrodes, and the DC bias voltage of 1 V has been applied to the setup in order to analyse the resulting polarization current as a function of time [7]. Figure 10 ascribes the plot of DC polarization current with respect to time. At first, the initial current is noted and, as a function of time, the current decreases and reaches the constant depleted state which is taken as the final current. Using initial current (I_i) and final current (I_f), the transference number of charge carriers is calculated using the formula [8]

$$t_{ion} = \frac{I_i - I_f}{I_i} \quad (5)$$

$$t_{elec} = \frac{I_f}{I_i} \quad (6)$$

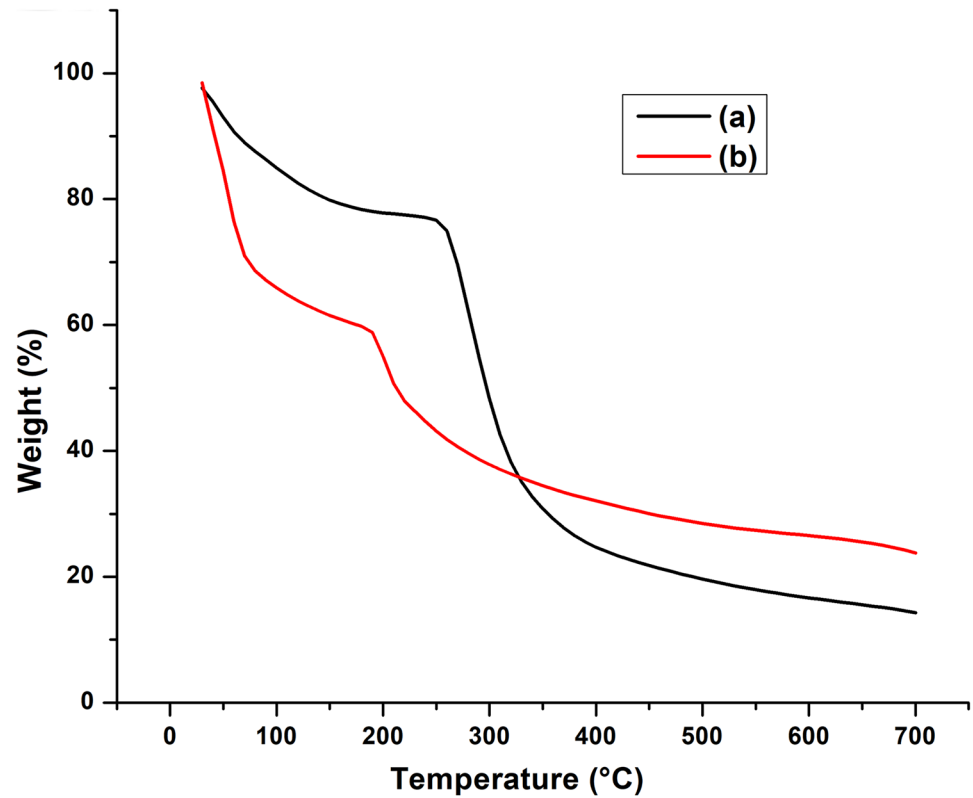
The transference number of ions (t_{ion}) is 0.98, and that of an electron (t_{elec}) is 0.02. From this, it is assured that the

majority of charge conduction is due to ions with negligible electronic conduction.

Evan's polarization method

Evan's polarization technique is done to measure the cationic transference number of the optimized highest ion conducting electrolyte (20 mol% of AA:80 mol% of LiCl). In the present study, the highest ion conducting electrolyte is placed between two silver electrodes with the configuration of Y (silver electrode) || X (high ion conducting electrolyte) || Y (silver electrode) and a small amount of DC voltage (V) is applied to the cell [41]. Then, the resulting initial (I_0) and final (I_s) currents are noted and the plot representing the change in current with respect to time is shown in Fig. 11. Also, AC impedance analysis has been carried out with the arranged setup in order to calculate the resistances before (R_0) and after (R_s) polarization. Figure 12a, b depicts the impedance plots before and after polarization of the cell. The value of cationic transference number is calculated using the following equation [18]:

Fig. 9 Thermograms of (a) pure agar (AA) (1 g) and (b) 20 mol% of AA:80 mol% of LiCl



$$t_{\text{Li}^+} = \frac{I_s(V - I_0R_0)}{I_0(V - I_sR_s)} \quad (7)$$

The value of cationic transference number obtained for the membrane with the composition of 20 mol% of AA:80 mol% of LiCl is 0.67. From this, it is guaranteed

Fig. 10 Variation in current with respect to time (Wagner's polarization method)

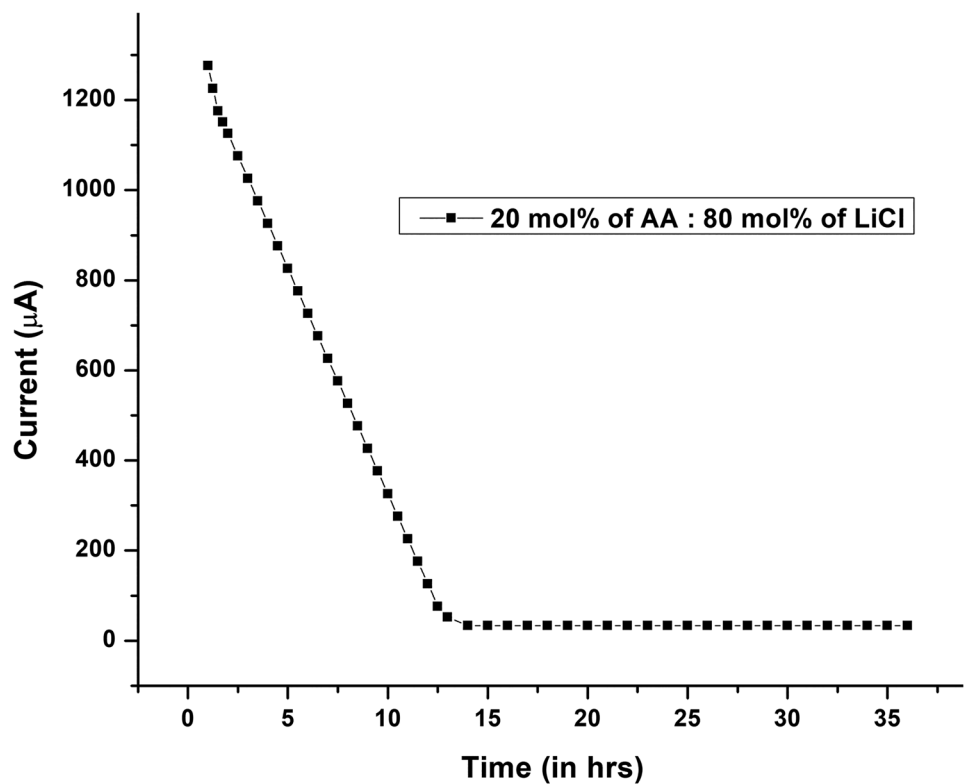
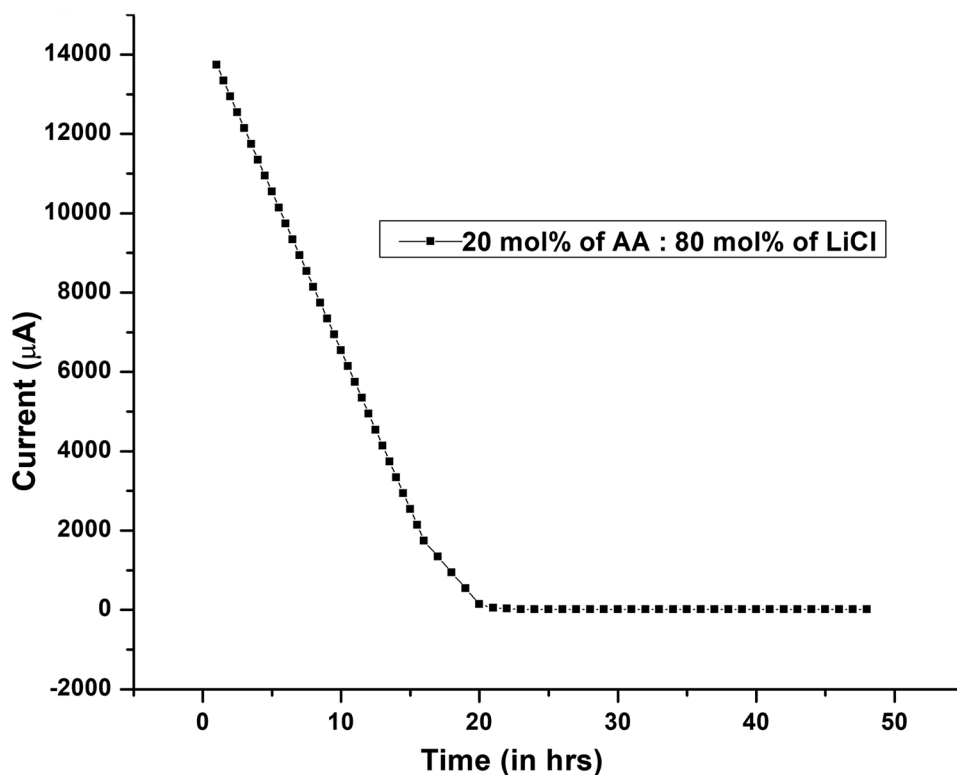


Fig. 11 Variation in current as a function of time (Evan's polarization method)



that the lithium-ion (Li^+) conduction is dominant in the electrolyte, resulting in high ionic conductivity. Chitra et al. [42], have reported lithium-ion conduction of 0.55 for 1.0 g I-carrageenan/0.5 wt% of LiClO_4 , and Arockia Mary et al. [11], have shown 0.58 of lithium-ion transference number for 1 g K-carrageenan with 0.65 wt% of LiNO_3 .

Cyclic voltammetry analysis

CV analysis has been carried out to examine the cycling stability of prepared electrolyte [18]. In the current work, the cycling performance of the highest ion conducting electrolyte with the composition of 20 mol% of AA:80 mol%

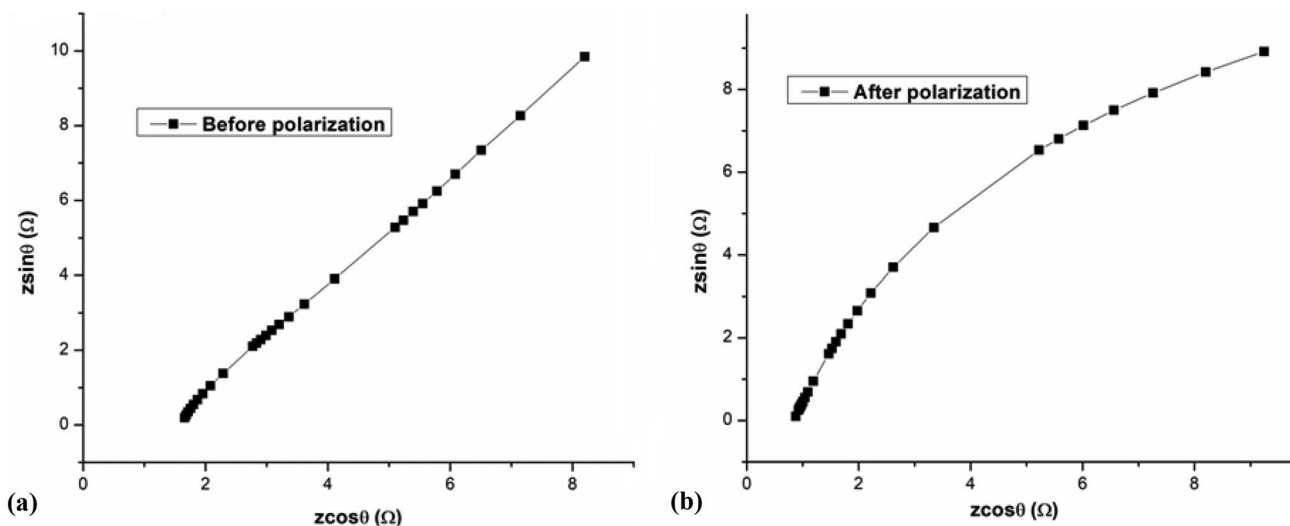
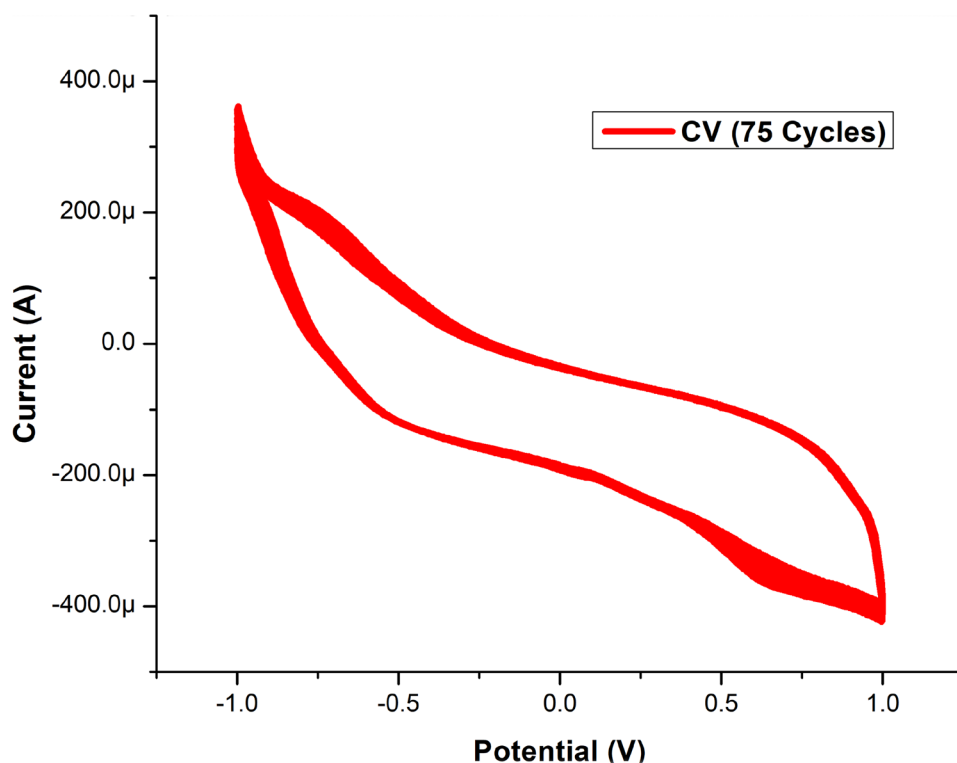


Fig. 12 Impedance plot of the highest ion conducting membrane (20 mol% of AA:80 mol% of LiCl). **a** Before polarization. **b** After polarization

Fig. 13 CV pattern of the highest ion conducting membrane (20 mol% of AA:80 mol% of LiCl)



of LiCl is analysed with the two-electrode system under the scan rate of 0.1 Vs^{-1} and the potential range fixed between -1 and $+1 \text{ V}$. Figure 13 shows the reciprocated CV pattern of the membrane (20 mol% of AA:80 mol% of LiCl) with high ionic conductivity. The obtained result with superior cycling stability of 75 cycles without much fluctuation in its sweep area indicates the better reversibility of an electrolyte. Subsequently, the process of redox reaction

takes place, whereas the oxidation occurs in anode and the reduction happens in cathode.

Primary Li-ion conducting battery

In the present work, the highest ion conducting membrane with the composition of 20 mol% of AA:80 mol% of LiCl has been utilized as an electrolyte in the fabrication of primary Li-ion conducting battery. The electrodes are made into thin pellets, whereas the anode is prepared with the composition of Zn metal powder (Zn) (8 g), $\text{ZnSO}_4 \cdot 7\text{H}_2\text{O}$

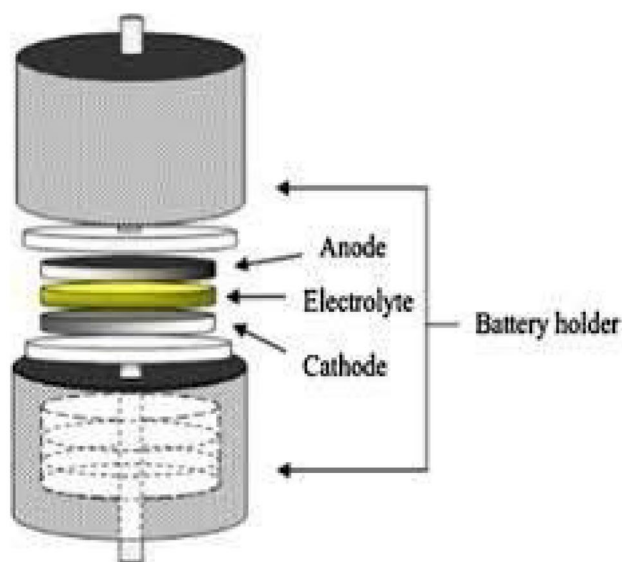


Fig. 14 Representation of constructed solid-state battery

Table 7 Important cell parameters of the optimized highest ion conducting membrane

Cell parameters	Values obtained for 20 mol% of AA:80 mol% of LiCl
Open-circuit voltage (V)	1.93
Current drawn (μA)	19
Weight of the cathode (g)	0.707
Weight of the anode (g)	0.852
Weight of the electrolyte (g)	0.111
Weight of the cell (g)	1.670
Thickness of the anode (mm)	1.523
Thickness of the cathode (mm)	1.672
Area of the cell (cm^2)	1.85
Discharge time (h)	72
Current density ($\mu\text{A}/\text{cm}^2$)	10.27

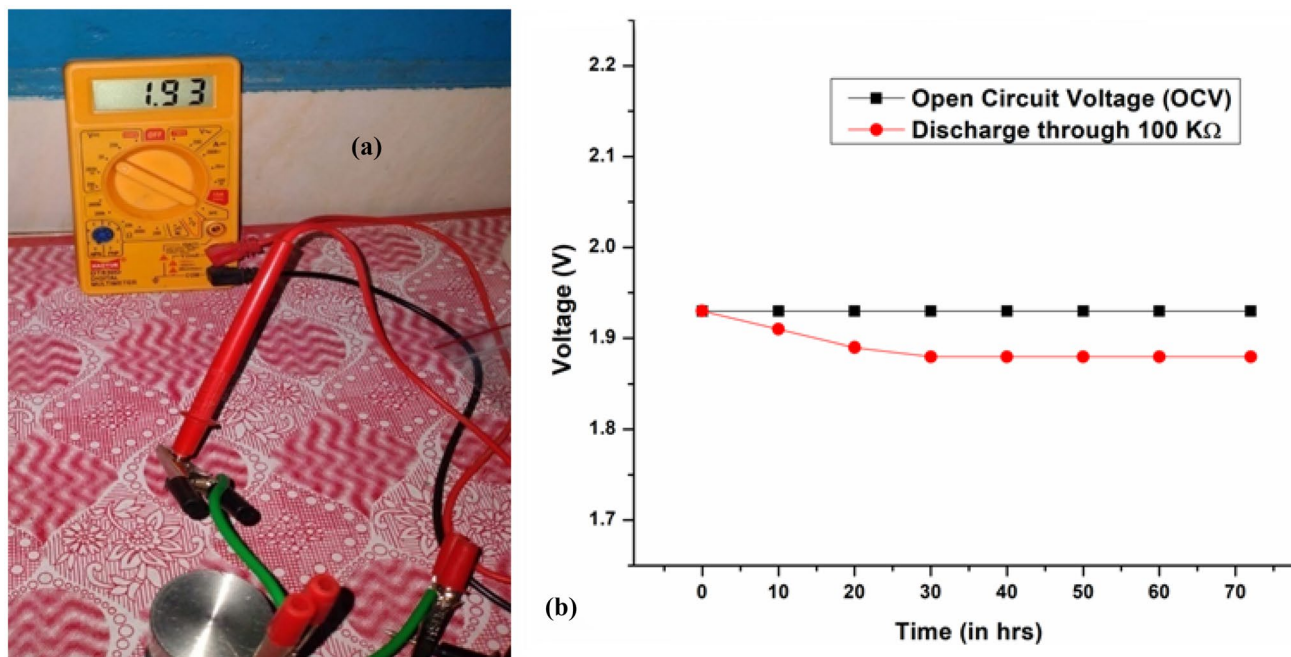
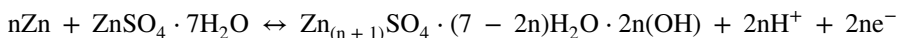


Fig. 15 a Open-circuit voltage (OCV) of fabricated cell and b plot describing the discharge characteristics of the cell (voltage (V) vs time (in h))

(2 g) and graphite powder (C) (1 g) followed by the cathode preparation with the composition of PbO₂ (3 g), V₂O₅ (1 g), graphite powder (1 g) and a piece of the highest ion conducting membrane (0.25 g), respectively. Subsequently, the cell is fabricated by sandwiching the highest ion conducting electrolyte between the anode and the cathode as



Zn + ZnSO₄·7H₂O + C || 20 mol% of AA:80 mol% of LiCl || PbO₂ + V₂O₅ + C + BPE and the arrangement is also shown in Fig. 14 [8].

The anode and cathode reaction is mentioned in the following [12, 43]:

Anode reaction is

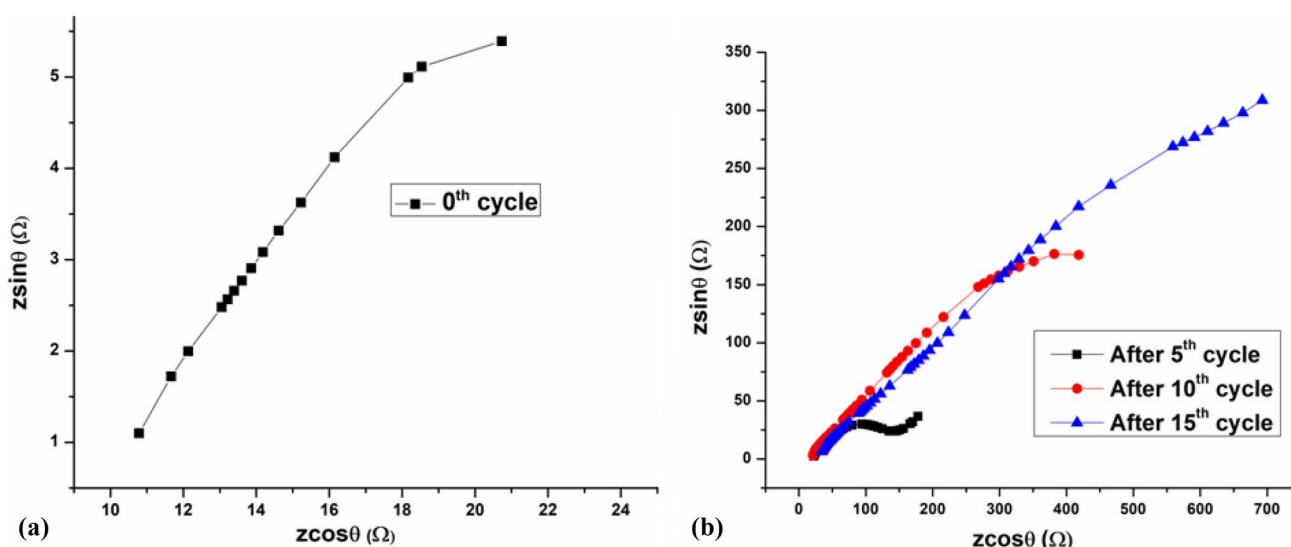
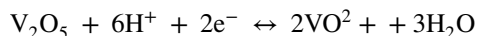
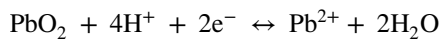


Fig. 16 Cole–Cole plot for a the 0th cycle and b the 5th, 10th and 15th cycles

Table 8 The resistance value measured for different cycles

Number of cycle	Resistance (Ω)
0	25
5	151
10	484
15	649

Cathode reaction is



Now, on the basis of hopping mechanism, the H^+ ions in the anode site repel the Li^+ ions in the electrolyte to the cathode site which results with an open-circuit voltage of 1.93 V. Figure 15a shows the OCV of fabricated cell. Then, a load 100 k Ω is applied to the constructed cell which shows a voltage drop of 1.88 V with 19 μA current drawn and the setup has been retained for 72 h. Figure 15b depicts the discharge characteristics of the cell as a function of time. Similar works based on fabrication of Li-ion conducting battery have been carried out by Chitra et al. [12] in “Synthesis and characterization of iota-carrageenan solid biopolymer

**Fig. 17** Initial voltage of the fabricated cell

electrolytes for electrochemical applications”, Arockia Mary et al. [11] in “Lithium ion conducting biopolymer membrane based on K-carrageenan with LiNO_3 ” and Aafrin Hazaana et al. [18] in “Development and characterization of biopolymer electrolyte based on gellan gum (GG) with lithium chloride (LiCl) for the application of electrochemical devices”. The examined cell parameters are listed in Table 7.

Rechargeable Li-ion conducting battery

In the current work, the optimized highest Li-ion conducting membrane with the composition of 20 mol% of AA:80 mol% of LiCl has been used as an electrolyte and the cell has been fabricated with the configuration of graphite (3 g) || 20 mol% of AA:80 mol% of LiCl (electrolyte) || LiFePO_4 (3 g) + graphite (1 g), respectively. The rechargeable nature of the membrane of the fabricated cell is analysed by charging and discharging the cell. The resistance nature of the cell for the 0th, 5th, 10th and 15th charge–discharge cycle has been measured from AC impedance analysis using the Cole–Cole plot, and the plots are depicted in Fig. 16a and b. The resistance measured before charging (0th cycle) is 25 Ω . After the 5th charge–discharge cycle, the resistance has been increased to 151 Ω , and subsequently, after the 10th cycle, the resistance measured is 484 Ω . After the 11th cycle, various loads have been applied and the resistance measured at the end of the 15th cycle is 649 Ω . The resistance observed for different cycles is listed in Table 8. Due to the lithium-ion deposition in the anode, the interfacial resistance is increased after various cycles.

The initial voltage measured for the constructed cell before charging (0th cycle) is 0.20 V (Fig. 17). Then, the cell has been charged for 3 h with the constant DC supply voltage of 3 V and then allowed to self-discharge for 3 h. The output characteristics of the cell after each cycle have been noted and the plot representing the voltage obtained for each cycle is given in Fig. 18. After continuous charge and discharge, the maximum voltage of 2.62 V has been obtained at the 10th cycle. The increased voltage is due to the more number of Li-ion that gets into the pores of

Table 9 Charge–discharge characteristics of the constructed cell (with load) and current drawn for each cycle

Number of cycle	Load (Ω)	Current (mA)	Voltage (V)	
			Charge (V)	Discharge (V)
11	100 k	0.026	2.56	0.30
12	47 k	0.059	2.56	0.31
13	10 k	0.253	2.55	0.31
14	4.7 k	0.451	2.55	0.29
15	150	15.512	2.51	0.28

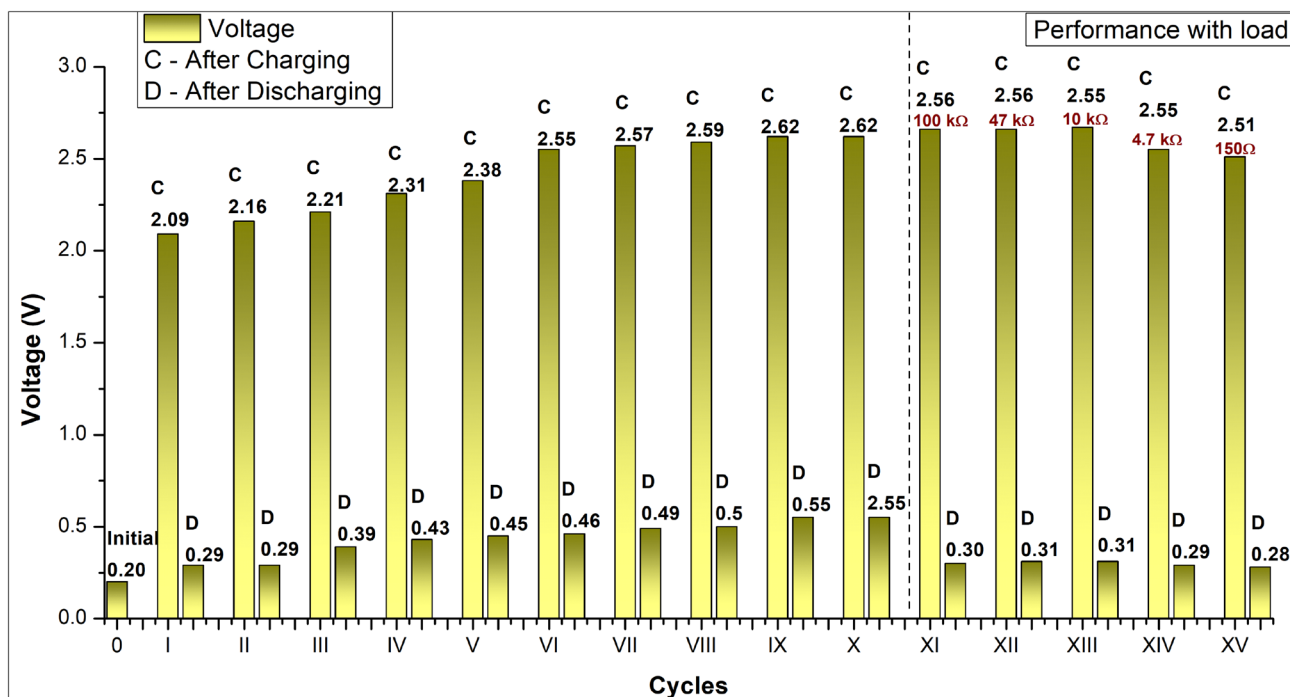


Fig. 18 Charge–discharge characteristics of the constructed cell

anode. If you increase the cycle more and more, the battery voltage could be increased further because more Li-ion could enter into the pores of anode (graphite). This process reveals that the membrane could be used as an electrolyte for rechargeable battery. From the 11th cycle to the 15th cycle, various loads of 100 kΩ, 47 kΩ, 10 kΩ, 4.7 kΩ and 150 Ω have been applied to the cell and the resulting voltage and current value have been observed (Fig. 18) and are depicted in Table 9. Therefore, the charge–discharge characteristics of the fabricated cell ensure the rechargeable nature of the prepared biopolymer electrolyte.

Conclusion

The biopolymer electrolytes based on agar–agar and LiCl have been prepared using solution casting method and are characterized using various characterization techniques. XRD is done to examine the crystalline/amorphous nature of prepared BPEs, and the membrane with the composition of 20 mol% of AA:80 mol% of LiCl shows high amorphous nature in contrast to other salt-added membranes. FTIR has been carried out to confirm the complex formation between the host biopolymer and salt. DSC is performed to examine the glass transition temperature of prepared BPEs, and the membrane 20 mol% of AA:80 mol% of LiCl gives a less T_g value of 37 °C which ensures the weak transient cross linkage between the OH⁻ of the polymer

and the cation (Li⁺) of the salt. The ionic conductivity of the prepared electrolytes is calculated using AC impedance analysis, and the membrane with the composition of 20 mol% of AA:80 mol% of LiCl resulted with a high ionic conductivity of $3.12 \pm 0.11 \times 10^{-2}$ S/cm. The highest ionic conductivity of the membrane may be due to high amorphous nature (confirmed by XRD) and low glass transition temperature (confirmed by DSC). SEM images are taken to analyse the surface morphology of prepared BPEs. TGA has been carried out to observe the thermal stability of prepared BPEs. The transference number measurement is performed to validate the conduction is mainly due to ions and the highest ion conducting membrane is calculated with the transference number of 0.98. CV has been carried out to evaluate the cyclic stability of the highest ion conducting membrane (20 mol% of AA:80 mol% of LiCl), and it also resulted with better cycling performance of 75 cycles without much fluctuation in its sweep area which confirms the reversibility of an electrolyte. Using the optimized highest ion conducting membrane (20 mol% of AA:80 mol% of LiCl), the Li-ion conducting primary battery has been fabricated and resulted with an OCV of 1.93 V. And, the rechargeable nature of the highest Li-ion conducting membrane (20 mol% of AA:80 mol% of LiCl) has been analysed by the charge–discharge characteristics of the fabricated cell. This study confirms that the membrane 20 mol% of AA:80 mol% of LiCl could be used for rechargeable battery.

References

- Li C, Wang ZY, He ZJ, Li YJ, Mao J, Dai KH, Yan C, Zheng JC (2021) An advance review of solid-state battery: challenges, progress and prospects. *Sustain Mater Technol* 29:e00297
- Yao P, Yu H, Ding Z, Liu Y, Lu J, Lavorgna M, Wu J, Liu X (2019) Review on polymer-based composite electrolytes for lithium batteries. *Front Chem* 7:522
- Zhao Q, Stalin S, Zhao CZ, Archer LA (2020) Designing solid-state electrolytes for safe, energy-dense batteries. *Nat Rev Mater* 5(3):229–252
- Gaele MF, Migliardini F, Di Palma TM (2021) Dual solid electrolytes for aluminium-air batteries based on polyvinyl alcohol acidic membranes and neutral hydrogels. *J Solid State Electrochem* 25(4):1207–1216
- Manjuladevi R, Thamilselvan M, Selvasekarapandian S, Mangalam R, Premalatha M, Monisha S (2017) Mg-ion conducting blend polymer electrolyte based on poly (vinyl alcohol)-poly (acrylonitrile) with magnesium perchlorate. *Solid State Ion* 308:90–100
- Qiu J, Yang L, Sun G, Yu X, Li H, Chen L (2020) A stabilized PEO-based solid electrolyte via a facile interfacial engineering method for a high voltage solid-state lithium metal battery. *Chem Commun* 56(42):5633–5636
- Chandra MV, Karthikeyan S, Selvasekarapandian S, Pandi DV, Monisha S, Packiaseli SA (2016) Characterization of high ionic conducting PVAc–PMMA blend-based polymer electrolyte for electrochemical applications. *Ionics* 22(12):2409–2420
- Naachiyar RM, Ragam M, Selvasekarapandian S, Krishna MV, Buvaneshwari P (2021) Development of biopolymer electrolyte membrane using gellan gum biopolymer incorporated with NH_4SCN for electro-chemical application. *Ionics* 27(8):3415–3429
- Vanitha N, Shanmugapriya C, Selvasekarapandian S, Naachiyar RM, Krishna MV, Aafrin Hazaana S, Nandhini K, Ramaswamy M (2022) Effect of graphene quantum dot on sodium alginate with ammonium formate (NH_4HCO_2) biopolymer electrolytes for the application of electrochemical devices. *Ionics* 28(6):2731–2749
- Kiruthika S, Malathi M, Selvasekarapandian S, Tamilarasan K, Moniha V, Manjuladevi R (2019) Eco-friendly biopolymer electrolyte, pectin with magnesium nitrate salt, for application in electrochemical devices. *J Solid State Electrochem* 23(7):2181–2193
- Arockia Mary I, Selvanayagam S, Selvasekarapandian S, Chitra R, Chandra L, Ponraj T (2020) Lithium ion conducting biopolymer membrane based on K-carrageenan with LiNO_3 . *Ionics* 26(9):4311–4326
- Chitra R, Sathya P, Selvasekarapandian S, Monisha S, Moniha V, Meyvel S (2019) Synthesis and characterization of iota-carrageenan solid biopolymer electrolytes for electrochemical applications. *Ionics* 25(5):2147–2157
- Selvalakshmi S, Mathavan T, Selvasekarapandian S, Premalatha M (2018) Effect of ethylene carbonate plasticizer on agar-agar: NH_4Br -based solid polymer electrolytes. *Ionics* 24(8):2209–2217
- Raphael E, Avellaneda CO, Manzolli B, Pawlicka A (2010) Agar-based films for application as polymer electrolytes. *Electrochim Acta* 55(4):1455–1459
- Ramnani P, Chitarrari R, Tuohy K, Grant J, Hotchkiss S, Philp K, Campbell R, Gill C, Rowland I (2012) In vitro fermentation and prebiotic potential of novel low molecular weight polysaccharides derived from agar and alginate seaweeds. *Anaerobe* 18(1):1–6
- Pandya YH, Bakshi M, Sharma A, Pandya H (2022) Agar-agar extraction, structural properties and applications: a review. *Pharma Innov J* 11:1151–1157
- Perumal P, Christopher Selvin P, Selvasekarapandian S (2018) Characterization of biopolymer pectin with lithium chloride and its applications to electrochemical devices. *Ionics* 24(10):3259–3270
- Aafrin Hazaana S, Joseph A, Selvasekarapandian S, Meera Naachiyar R, Vengadesh Krishna M, Muniraj Vignesh N (2022) Development and characterization of biopolymer electrolyte based on gellan gum (GG) with lithium chloride (LiCl) for the application of electrochemical devices. *Polym Bull* pp. 1–21
- Suvarna K, Kirubavathy SJ, Selvasekarapandian S, Krishna MV, Ramaswamy M (2022) Corn silk extract-based solid-state biopolymer electrolyte and its application to electrochemical storage devices. *Ionics* 28(4):1767–1782
- Venkata Jyotsna R, Vengadesh Krishna M, Chandrasekar P, Monisha S (2022) Fabrication of rechargeable lithium ion coin cell using a biopolymer electrolyte (cellulose acetate). In *Proceedings of Fourth International Conference on Inventive Material Science Applications* (pp. 559–568). Springer, Singapore
- Arockia Mary I, Selvanayagam S, Selvasekarapandian S, Chitra R, Krishna MV, Monisha S (2022) Lithium ion conducting biopolymer membrane based on kappa carrageenan with LiCl and its application to electrochemical devices. *Mater Today: Proc* 58:855–861
- Boopathi G, Pugalendhi S, Selvasekarapandian S, Premalatha M, Monisha S, Aristatil G (2017) Development of proton conducting biopolymer membrane based on agar-agar for fuel cell. *Ionics* 23(10):2781–2790
- Hodge RM, Edward GH, Simon GP (1996) Water absorption and states of water in semicrystalline poly (vinyl alcohol) films. *Polymer* 37(8):1371–1376
- Guerrero P, Etxabide A, Leceta I, Peñalba M, De la Caba K (2014) Extraction of agar from *Gelidium sesquipedale* (Rodhopyta) and surface characterization of agar based films. *Carbohydr Polym* 99:491–498
- Sekkal M, Huvenne JP, Legrand P, Sombret B, Mollet JC, Mouradi-Givernaud A, Verdu MC (1993) Direct structural identification of polysaccharides from red algae by FTIR microspectrometry I: localization of agar in *Gracilaria verrucosa* sections. *Microchim Acta* 112(1):1–10
- Gómez-Ordóñez E, Rupérez P (2011) FTIR-ATR spectroscopy as a tool for polysaccharide identification in edible brown and red seaweeds. *Food Hydrocoll* 25(6):1514–1520
- Selvalakshmi S, Vijaya N, Selvasekarapandian S, Premalatha M (2017) Biopolymer agar-agar doped with NH_4SCN as solid polymer electrolyte for electrochemical cell application. *J Appl Polym Sci* 134(15)
- Muthukrishnan M, Shanthi C, Selvasekarapandian S, Manjuladevi R, Perumal P, Christopher Selvin P (2019) Synthesis and characterization of pectin-based biopolymer electrolyte for electrochemical applications. *Ionics* 25(1):203–214
- Boukamp BA (1986) A package for impedance/admittance data analysis. *Solid State Ion* 18:136–140
- Perumal P, Selvin PC, Selvasekarapandian S, Sivaraj P (2019) Structural and electrical properties of bio-polymer pectin with LiClO_4 solid electrolytes for lithium ion polymer batteries. *Mater Today: Proc* 8:196–202
- Kumar LS, Selvin PC, Selvasekarapandian S (2021) Impact of lithium triflate (LiCF_3SO_3) salt on tamarind seed polysaccharide-based natural solid polymer electrolyte for application in electrochemical device. *Polym Bull* 78(4):1797–1819
- Nirmala Devi G, Chitra S, Selvasekarapandian S, Premalatha M, Monisha S, Saranya J (2017) Synthesis and characterization of dextrin-based polymer electrolytes for potential applications in energy storage devices. *Ionics* 23(12):3377–3388
- Kumar S, Boro JC, Ray D, Mukherjee A, Dutta J (2019) Bionanocomposite films of agar incorporated with ZnO nanoparticles as an active packaging material for shelf life extension of green grape. *Heliyon* 5(6):e01867
- Genova KM, F., Selvasekarapandian, S., Vijaya, N., Sivadevi, S., Premalatha, M. and Karthikeyan, S. (2017) Lithium ion-conducting

- polymer electrolytes based on PVA–PAN doped with lithium triflate. *Ionics* 23(10):2727–2734
35. Baskaran R, Selvasekarapandian S, Kuwata N, Kawamura J, Hattori T (2007) Structure, thermal and transport properties of PVAc–LiClO₄ solid polymer electrolytes. *J Phys Chem Solids* 68(3):407–412
 36. Ouyang QQ, Hu Z, Li SD, Quan WY, Wen LL, Yang ZM, Li PW (2018) Thermal degradation of agar: mechanism and toxicity of products. *Food Chem* 264:277–283
 37. Alves RD, Rodrigues LC, Andrade JR, Pawlicka A, Pereira L, Martins R, Fortunato E, Silva MM (2013) Study and characterization of a novel polymer electrolyte based on agar doped with magnesium triflate. *Mol Cryst Liq Cryst* 570(1):1–11
 38. Naachiyar MR, Ragam M, Selvasekarapandian S, Aristatil G, Hazaana AS, Vignesh MN, Krishna VM (2022) Fabrication of rechargeable proton battery and PEM fuel cell using biopolymer gellan gum incorporated with NH₄HCO₂ solid electrolyte. *J Polym Res* 29(8)
 39. Vanitha N, Shanmugapriya C, Selvasekarapandian S, Krishna MV, Nandhini K (2022) Investigation of N–S-based graphene quantum dot on sodium alginate with ammonium thiocyanate (NH₄SCN) biopolymer electrolyte for the application of electrochemical devices. *J Mater Sci Mater Electron* pp. 1–21
 40. Machado GDO, Regiani AM, Pawlicka A (2003) Carboxymethyl-cellulose derivatives with low hydrophilic properties. *Polimery* 48(4):273–279
 41. Diana MI, Selvin PC, Selvasekarapandian S, Krishna MV (2021) Investigations on Na-ion conducting electrolyte based on sodium alginate biopolymer for all-solid-state sodium-ion batteries. *J Solid State Electrochem* 25(7):2009–2020
 42. Chitra R, Sathya P, Selvasekarapandian S, Meyvel S (2020) Synthesis and characterization of iota-carrageenan biopolymer electrolyte with lithium perchlorate and succinonitrile (plasticizer). *Polym Bull* 77(3):1555–1579
 43. Aafrin Hazaana S, Ancemma J, Selvasekarapandian S (2022) Efficacy of graphene quantum dot on gellan gum based biopolymer electrolyte for the application of solid state battery. *Int J Nanomater Nanotechnol Nanomedicine* 4(1) (Short communication)

Publisher's Note Springer Nature remains neutral with regard to jurisdictional claims in published maps and institutional affiliations.

Springer Nature or its licensor (e.g. a society or other partner) holds exclusive rights to this article under a publishing agreement with the author(s) or other rightsholder(s); author self-archiving of the accepted manuscript version of this article is solely governed by the terms of such publishing agreement and applicable law.